ELSEVIER

European Journal of Pharmaceutics and Biopharmaceutics 43 (1997) 73–81

European Journal of Pharmaceutics and Biopharmaceutics

Interaction and translocation of cysteamine (mercaptoethylamine) with model membranes: a ^{15}N-NMR and ^{1}H-NMR study

Catherine Lagoueyte[a], Guy Subra[a], Pierre-Antoine Bonnet[a,*], Jean-Pierre Chapat[a], Jean-Claude Debouzy[b], Florence Fauvelle[b], François Berleur[b], Vincent Roman[b], Marc Fatome[b], Jean-Paul Fernandez[c]

[a] *URA-CNRS 1111, Faculté de Pharmacie, 15, Av. Ch. Flahault, 34060 Montpellier, Cedex, France*
[b] *Centre de Recherches du Service de Santé des Armées, 38700 La Tronche, France*
[c] *CRBM-CNRS, 34000 Montpellier, Cedex, France*

Received 3 April 1995; accepted 1 August 1996

Abstract

We investigated by ^{15}N-NMR (nuclear magnetic resonance) spectroscopy the interactions of ^{15}N-labeled cysteamine ([^{15}N]mercaptoethylamine (MEA)), a radioprotecting aminothiol, with model membranes of egg yolk phosphatidylcholine (EPC) and phosphatidic acid (EPA). We prepared large unilamellar vesicles (LUVs) with a pH gradient between the intravesicular space and the bulk medium. Over the pH range from 4.8 to 8.1, the observations show a MEA incorporation into the vesicles. This result is consistent with a specific dissociation balance at the lipid–water interface. We carried out another ^{1}H-NMR experiment with unlabeled MEA in the presence of small unilamellar vesicles (SUVs). It revealed that the interactions of MEA within the hydrophobic core of the phospholipidic bilayer vary with external pH value over the range 4.0–7.1. Through these experiments, and others compiled from the literature, it was concluded that ^{15}N-NMR spectroscopy is particularly successful for transmembrane transport analysis.

Keywords: Cysteamine; ^{1}H-NMR; Mercaptoethylamine; Model membrane; ^{15}N-NMR; pH; Transmembrane transport; Vesicles

1. Introduction

In liposomal systems, cross-membrane translocation of various weak bases, especially lipophilic amine, or even of acids, has been demonstrated under a transmembrane pH gradient [1–3]. Most studies imply a separation and a disruption of the vesicles after translocation of the drug, prior to measuring the incorporated fraction. In some in situ studies, the extra- or intravesicular location of the drug has been determined by fluorescence modulation. For translocation of proteins or peptides across model or biological membranes, some analyses used labeled molecules either by fluorescent dyes such as 7-nitrobenz-2-oxa-1,3-diazolyl (NBD) or dansyl groups. In these cases, the attachment of a bulky group on the molecule may result in artifacts.

To study directly, in biological systems, the translocation of a small molecule, nuclear magnetic resonance (NMR) spectroscopy methods are unique, in that they can be performed in situ. The change of a specific isotope (^{2}H, ^{13}C, ^{15}N, or so) is not invasive.

Some authors have investigated transmembrane transport of phosphotriester compounds by using ^{31}P-NMR on large unilamellar vesicles (LUVs) as model membranes [4–6]. During their preparation, LUVs can

Abbreviations: DPPC, dipalmitoylphosphatidylcholine; EPA, egg yolk phosphatidic acid; EPC, egg yolk phosphatidylcholine; ESR, electron spin resonance; LUV, large unilamellar vesicle; MEA, mercaptoethylamine (cysteamine); NMR, nuclear magnetic resonance; SUV, small unilamellar vesicle.

* Corresponding author: Tel./fax: + 33 04 67 543814.

0939-6411/97/$17.00
PII S0939-6411(96)00012-4

enclose a significant volume of solution. Paramagnetic ions such as Mn^{2+}, that do not cross bilayers, perturb specifically the signal from the extravesicular medium. Thus, the combined use of LUVs and Mn^{2+} allows the observation of ^{31}P-NMR signal changes, due to the molecules that undergo a transmembrane transport.

In the present report, we used ^{15}N-NMR spectroscopy to analyze the influence of a pH gradient on the translocation of ^{15}N-labeled mercaptoethylamine across membrane bilayers [7].

^{1}H-NMR spectroscopy is also interesting with small unilamellar vesicles (SUVs), as another type of model membrane, to establish the location of various drugs within the lipid bilayers. ^{1}H-NMR spectroscopy has been used with molecules like ajoene or malonyldialdehyde and some anions [8–10]. This system displays resonances of 10–20 Hz line widths. Paramagnetic ions, confined outside, help to locate precisely the molecule interacting with the SUVs.

β-Mercaptoethylamine ($SH-CH_2-CH_2-NH_2$, cysteamine or MEA), was first identified as a hydrophilic radioprotector aminothiol in 1952 [11]. This polar molecule of low molecular weight, is considered as a standard among sulphur containing molecules. Its basic structure can be found in most radioprotective compounds of general formula:

$$H_2N-(CH_2)_n-NH-(CH_2)_m-SH.$$

Among the proposed radioprotection mechanisms for aminothiols, one hypothesis suggests a role in membrane protection, due to an inhibition of radioinduced lipid peroxidations [12,13]. Then, a radioprotective hypoxia of the living cell results from a decrease of oxygen diffusion across cell membrane upon MEA-phospholipid interactions [14]. The study of MEA (or other drugs) interactions with phospholipidic model membranes of LUVs or SUVs is also a powerful model for developing vectors for pharmacological drugs [14,15]. As an illustration, MEA and many radioprotectors are totally inactive when given orally. Incorporation of MEA into egg yolk lecithine liposomes had revealed a clear radioprotective property by oral route, due to a protection from digestive degradation [14,15]. In addition, the toxicity decreased.

In the present study, we used ^{15}N-NMR and ^{1}H-NMR spectroscopy on such model membranes to examine the interaction of MEA with lipid bilayers. In particular, we focused our attention on the role of a pH gradient between both sides of the model membrane, on the penetration and translocation of MEA. Such studies were designed to be easily generalized to other molecules bearing an amine group.

2. Materials and methods

2.1. MEA and lipids

MEA, unstable at pH > 7.0, is stored in the hydrochloride form. MEA hydrochloride was purchased from Fluka and 99% ^{15}N-labeled glycine from Eurisotop (Saint-Aubin, France). MEA ^{1}H-NMR resonances, referenced to tetramethylsilane, are found at 2.8 (CH_2SH) and 3.2 (CH_2NH_2) ppm in D_2O. The presence of thin resonances was in full agreement with the water-solubility of MEA.

^{15}N-labeled MEA hydrochloride was synthesized in our laboratory in six steps from [^{15}N]glycine [7]. Intermediate [^{15}N]ethanolamine is treated with an excess of propionic acid to obtain a [^{15}N]acylaminoalcohol which yields, after treatment with phosphorus pentasulfide, a [^{15}N]dihydrothiazole. Then, acidic hydrolysis gives 99% ^{15}N-labeled MEA hydrochloride whose purity was checked by ^{1}H-NMR.

Egg yolk phosphatidylcholine (EPC) (100 mg ml^{-1}) and egg yolk lecithin phosphatidic acid (EPA) sodium salt (10 mg ml^{-1}) were purchased from Fluka.

2.2. NMR experiments

All NMR experiments are carried out at 25°C on an AM-400WB Bruker spectrometer (9.4 T).

^{15}N-NMR experiments are performed using a broadband probe head tuned to 40.55 MHz. Chemical shifts are referenced in relation to NH_4Cl used as an external standard. Recordings are performed using single 60° pulses (14 μs duration) with composite proton decoupling during acquisition time. By using an 8000 Hz spectral width, 2500 or 3000 scans are averaged in quadrature mode detection. All spectra are obtained during an acquisition time of 2.49 s and with a recycling delay of 16 s.

^{1}H-NMR experiments are recorded at 400 MHz using the ^{1}H channel of the same broadband high resolution reverse probe of 5 mm (Spectral width: 4000 Hz, Recycling delay: 1 s, line broadening: 1 Hz). Chemical shifts are referenced in relation to *d4*-TSP (sodium 2,2,3,3-tetradeuterio-3-(trimethylsilyl)propionate) in water as external reference.

^{31}P-NMR experiments are performed at 161 MHz with a broadband proton decoupling using composite pulse decoupling to avoid heating the sample. Chemical shifts are referenced in relation to phosphoric acid.

2.3. Vesicle preparation

LUVs of defined size are prepared in a pH 4.8 phosphate buffer (Na_2HPO_4/KH_2PO_4 67 mM) by reverse-phase evaporation, as described by Szoka and Papahadjopoulos [16]. A mixture of EPC and EPA

(EPC/EPA molar ratio 9:1) ensures a good stability of the vesicles. This suspension is sequentially extruded through 800, 400 and 200 nm polycarbonate membranes (Nucleopore) to obtain a uniform size distribution [17]. The final lipid concentration is about 20 mM. LUV integrity is analyzed by recording a 161 MHz ^{31}P-NMR spectrum of a blank sample of vesicles. The chemical shift of ^{31}P-resonance from the phosphate buffer can be directly related to the local pH, using pH titration curves [18–20]. The presence of a pH gradient (internal pH (pH_{int}) = 4.8 and external pH (pH_{ext}) = 7.5) gives two ^{31}P-NMR resonances. The downfield and upfield signals correspond to external and internal buffer phosphate respectively. The phospholipid phosphate signals are negligible, due to intrinsic width (1 kHz), low concentration and rapid relaxation rates. The ^{31}P-NMR spectrum of a LUV sample with pH_{int} and pH_{ext} 4.8 shows a single ^{31}P-resonance.

SUVs are prepared following Huang [21] by a 2 h sonication of EPC in a pH 4.0 phosphate buffer. The final lipid concentration is about 10 mM. SUV integrity is checked by a 400 MHz ^{1}H-NMR spectrum that presents 15 Hz lines for both terminal-CH_3 (0.8 ppm) and choline-CH_3 (3.2 ppm). Actually, vesicle disruption is easily discernible by ^{1}H-NMR either from the presence of new narrow resonances (2–3 Hz) due to small and mobile moieties or, conversely, from broad resonances ($\geq$ 100 Hz) imputable to the formation of aggregates following SUV coalescence [22]. Such modifications of ^{1}H-NMR spectra were never observed during the course of our experiments.

Fig. 1 shows a complete ^{1}H-NMR spectrum with assignments for egg phosphatidylcholine SUVs in D_2O. The major $-(CH_2)_n-$, $-CH_3$ and choline $-N^+(CH_3)_3$ resonances of phosphatidylcholine are clearly visible [22]. The choline $-CH_2N^+-$ and $-OPO_3CH_2-$ methylene protons resonate at 3.71 and 4.32 ppm, respectively. The *sn*-2 glycerol $-CHOCO-$ resonance overlaps the vinyl–CH=CH– resonance at approximately 5.3 ppm. Both the *sn*-1 glycerol methylene protons $-CH_2OCO-$ are not magnetically equivalent: the first ^{1}H is at 4.43 ppm and the second overlaps the high-field side of the choline–OPO_3CH_2- at 4.25 ppm. Both the *sn*-3 glycerol methylene protons $-CH_2OP-$ resonate in the wide signal at 4.02 ppm.

The extravesicular medium is then supplemented with a solution of paramagnetic $MnCl_2$ (0.1 M) to eliminate all the resonances of the external medium, as already described [18,23]. Upon Mn^{2+} addition, the vesicle integrity is preserved since terminal methyl groups still appear as $\approx$ 15 Hz linewidth resonances. Vesicle integrity is maintained for at least 2 days.

3. Results

3.1. ^{15}N-NMR experiments in LUV

^{15}N-NMR spectra of ^{15}N-MEA are recorded in the presence of LUVs, prior to, and after addition of Mn^{2+} ($MnCl_2$, 20 μl, 0.1 M). It is noteworthy that Mn^{2+} does not cross the bilayers and broadens the NMR signal of accessible ^{15}N beyond detection [18,23]. The only resonances detected are attributed to the resonances of molecules located in the intravesicular medium or within the inner leaflet. Another point to consider is that vesicle integrity is not affected by the presence of external Mn^{2+} since ^{31}P-NMR resonances arising from internal phosphorus are not modified [24,25]. ^{15}N-NMR studies are carried out with 2 mg of ^{15}N-MEA hydrochloride, added in the LUV extravesicular medium (molar ratio MEA/phospholipids = 6:5).

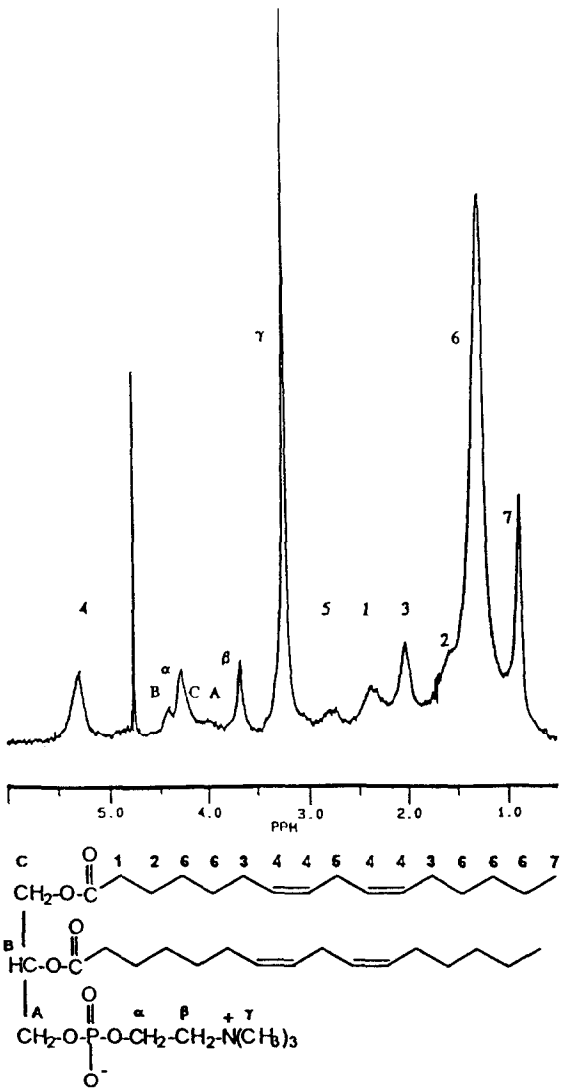

Fig. 1. 400 MHz ^{1}H-NMR spectra of SUV of EPC; the reference is set to HOD at 4.72 ppm; proton resonances are labeled as shown.

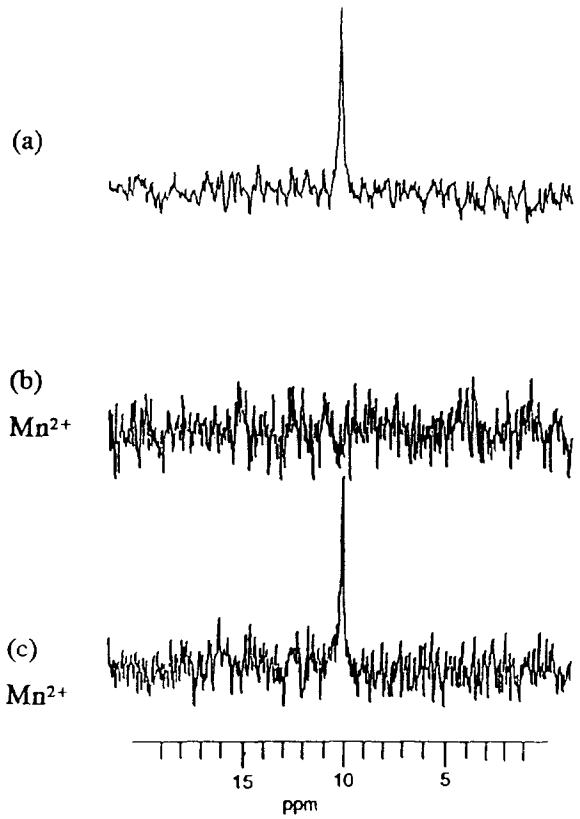

Fig. 2. 40.55 MHz ^{15}N-NMR spectra of ^{15}N-MEA-containing LUVs in the absence (a, NSa = 55) and in the presence (b, NSb = 45; c, NSc = 3000) of Mn^{2+}. The three spectra are recorded in the presence of LUVs whose initial $pH_{int} = pH_{ext} = 4.8$. Accumulation of scans allows the observation of a ^{15}N signal (c) even in absence of a pH gradient.

Initial pH_{int} of LUVs is 4.8 and pH_{ext} can be changed as desired.

Fig. 2a (55 scans) shows the ^{15}N-NMR spectrum of ^{15}N-MEA recorded in the presence of LUVs, at $pH_{int} = pH_{ext} = 4.8$. The spectrum shows a single line at 10 ppm. Addition of Mn^{2+} results in the loss of the signal (Fig. 2b, 45 scans). However, accumulating more scans still allows the detection of the line (Fig. 2c, 3000 scans). This result suggests that a part of ^{15}N-MEA may locate within the membrane bilayer and is able to cross. Peak areas are measured by integration and the percentage of ^{15}N-MEA that crossed the bilayer is evaluated as follows:

$$\% = I_c/I_a\sqrt{NSa/NSc}$$

where I_c and I_a are the peak areas; NSa and NSc are the number of scans, in Fig. 2a and c, respectively.

For LUVs with initial $pH_{int} = pH_{ext} = 4.8$, the percentage of ^{15}N-MEA present into the membrane and sheltered from Mn_2^+ is estimated around 8%.

Fig. 3a (50 scans) shows the one-line signal around 10 ppm, of ^{15}N-MEA recorded with LUVs at $pH_{int} = 4.8$ and $pH_{ext} = 6.45$. In spite of Mn^{2+}, the ^{15}N line is easily detectable (Fig. 3b, 250 scans and Fig. 3c, 2900 scans). Observing a line with a so few scans (250), suggests that incorporation of ^{15}N-MEA into the membrane is more important in presence of a pH gradient. Using the formula mentioned above, 13% of ^{15}N-MEA are estimated to have crossed the membrane and are no longer sensitive to Mn^{2+}.

Fig. 4a (174 scans) shows the ^{15}N lines of ^{15}N-MEA recorded at $pH_{int} = 4.8$ and $pH_{ext} = 8.1$. Yet, in spite of Mn^{2+}, the ^{15}N signal is observed with a few scans (Fig. 4b: 174 scans and Fig. 4c: 3600 scans). As seen above, at this pH gradient, 33% of ^{15}N-MEA is located in the vesicles.

All these results on ^{15}N-MEA interaction with LUVs are confirmed when analyzing Fig. 5. The three spectra are recorded with 170 scans. Initial pH_{int} is 4.8 and pH_{ext} are 4.8 (Fig. 5a); 6.45 (Fig. 5b) and 8.07 (Fig. 5c). For a given Mn^{2+} concentration, the higher the initial pH_{ext}, the higher the ^{15}N peak magnitude. Such results confirm the strong pH-dependent MEA-membrane interaction.

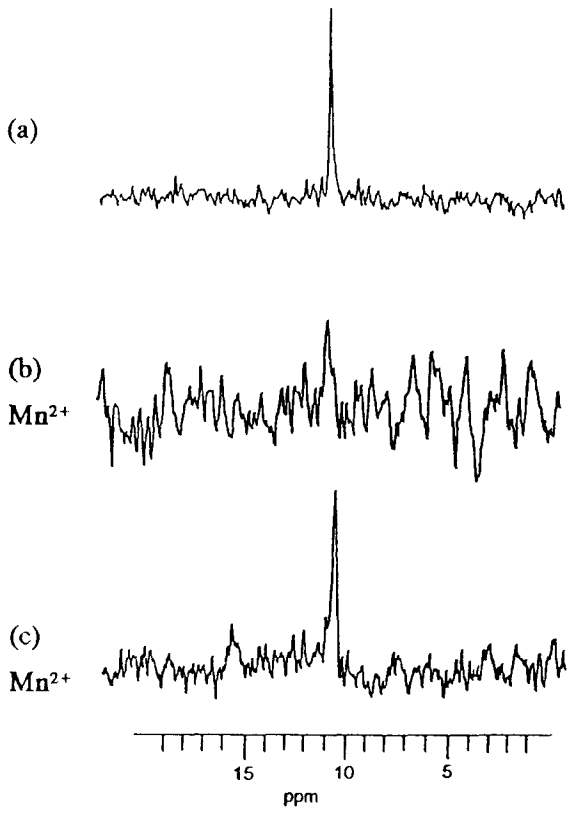

Fig. 3. 40.55 MHz ^{15}N-NMR spectra of ^{15}N-MEA-containing LUVs in the absence (a, NSa = 50) and in the presence (b, NSb = 250; c, NSc = 2900) of Mn^{2+}. The three spectra are recorded in the presence of LUVs whose initial $pH_{int} = 4.8$ and $pH_{ext} = 6.45$. Incorporation of ^{15}N-MEA into the membrane is more important in the presence than in the absence (b, presence of a ^{15}N signal as soon as NS = 250) of a pH gradient.

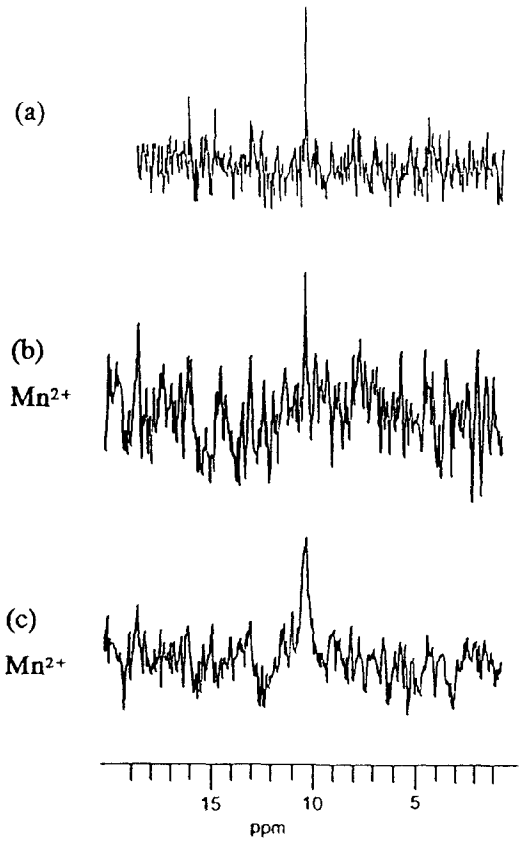

Fig. 4. 40.55 MHz ^{15}N-NMR spectra of ^{15}N-MEA-containing LUVs in the absence (a, NSa = 174) and in the presence (b, NSb = 174; c, NSc = 3600) of Mn^{2+}. The three spectra are recorded in the presence of LUVs whose initial $pH_{int} = 4.8$ and $pH_{ext} = 8.07$. As soon as NSb = NSa, incorporation of ^{15}N-MEA is clearly observed.

3.2. ^{1}H-NMR experiments in SUVs

^{1}H-NMR spectra are recorded after adding unlabeled MEA to a SUV suspension (molar ratio MEA–phospholipids: 1:4).

Fig. 6a shows a spectrum of SUVs in the presence of MEA and at initial $pH_{int} = pH_{ext} = 4.0$. Compared to the spectrum of pure SUVs, the phospholipid resonances are not affected by MEA. The chemical shifts of MEA resonances are the same as in aqueous solution. Only the upfield signals are clearly detected as the other ones are overlapped by the wide $-N^+(CH_3)_3$ signal (see line γ, Fig. 1). However, a broadening of MEA signals in the presence of SUVs suggests the existence of a MEA-membrane interaction.

To follow the broadening of the MEA resonances upon addition of Mn^{2+}, we increased amounts of $MnCl_2$ (from 2 to 14 μl of a 0.1 M solution) without pH gradient ($pH_{int} = pH_{ext} = 4.0$).

Fig. 6b shows MEA, phospholipid methyl, methylene, glycerol and choline resonances after 14 μl $MnCl_2$ addition. Every proton of the phospholipid polar moiety displays a separate resonance for each leaflet. Though a small amount of $MnCl_2$ would broaden the outer leaflet signal beyond any detection, the signal of the inner leaflet is not affected significantly [8,26]. Since for a given signal the product of the peak height by the half-width is a constant, we can follow the signal broadening by plotting the height of the peak vs. Mn^{2+} concentration. Thus, Fig. 7 shows a rapid decrease of the choline h/h_o ratio (Mn^{2+}-induced height on control height) at low Mn^{2+} concentration, followed by a plateau around 1/3. This value is consistent with the inner/outer phospholipid ratio and corresponds to a complete saturation of the system by Mn^{2+}. Besides, the protons of the terminal methyl group give a single line which is gradually broadened when increasing $MnCl_2$ concentration. Similarly, MEA resonances are progressively affected, but to a lesser extent. Mn^{2+} has the same effect on phospholipid methylene and methyl resonances. For both, peak magnitudes are reduced by 30%.

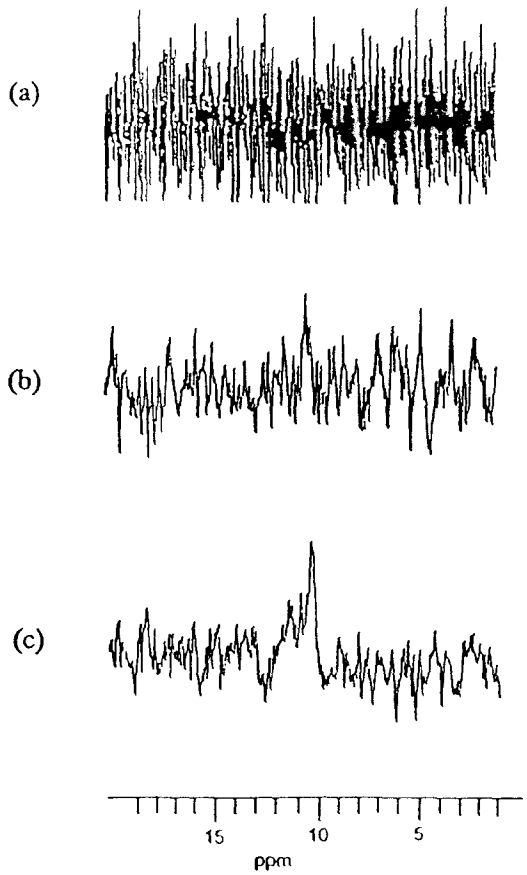

Fig. 5. 40.55 MHz ^{15}N-NMR spectra of ^{15}N-MEA-containing LUV upon $MnCl_2$ addition (20 μl 0.1 M) and for a number of scans identical for the three spectra (a–c) and always equal to 170. The three spectra are all recorded with initial $pH_{int} = 4.8$. and with variable initial pH_{ext} values: 4.8 (a), 6.45 (b), 8.1 (c). These spectra show that the higher the pH_{ext}, the more the ^{15}N-peak intensity increased for a given number of scans and a given $MnCl_2$ concentration.

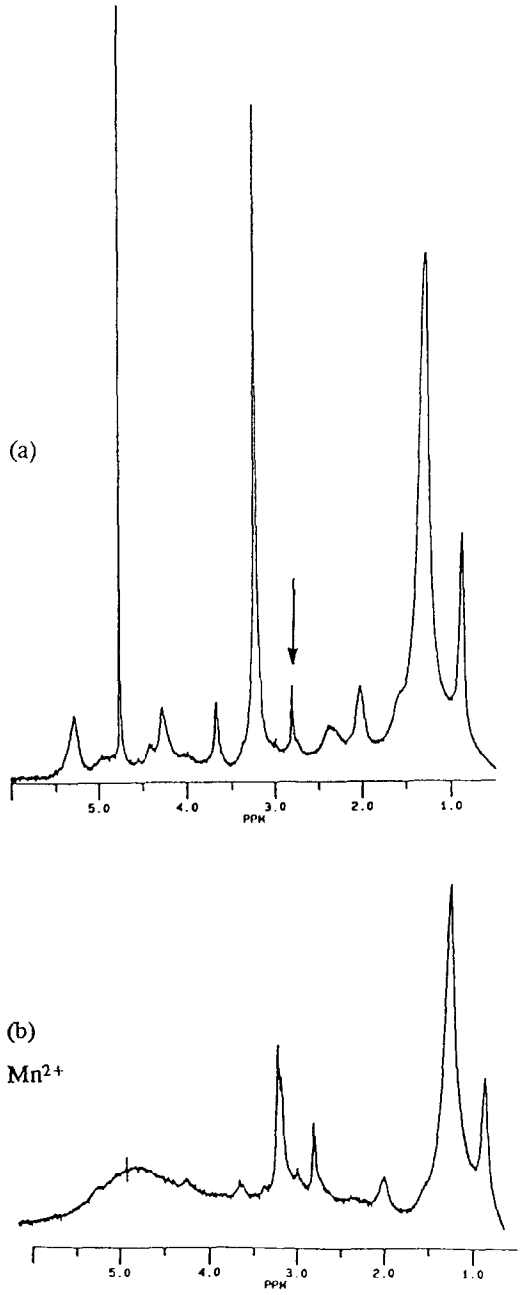

Fig. 6. 400 MHz ^{1}H-NMR spectra of MEA-containing SUVs. MEA/phospholipids molar ratio of 1:4. Both spectra are recorded in absence of a pH gradient, initial $pH_{int} = pH_{ext} = 4.0$. Highfield MEA resonances are pointed out by the arrow. Downfield resonances are lost in the $N^+(CH_3)_3$ peak. Prior to $MnCl_2$ addition (a), only the upfield resonances of MEA can be clearly observed. After 14 μl 0.1 M $MnCl_2$ addition (b), broadening of MEA resonance confirms the existence of a MEA-membrane interaction in absence of a pH gradient.

A similar study is carried out with an initial pH gradient: $pH_{int} = 4.0$ and $pH_{ext} = 7.8$. 1–5 μl of the 0.1 M $MnCl_2$ solution are added. Fig. 8 shows the spectrum for 5 μl and the results on MEA, methyl, methylene and choline are plotted in Fig. 9. When 1 μl is added, polar headgroup choline resonances are rapidly affected, whereas the lines attributed to alkyl groups are not. Thus, Mn^{2+} only affects the signals of the extravesicular molecules and the outer leaflet. MEA signal intensities are weakly but rapidly decreased by Mn^{2+} addition. In contrast with the previous study, MEA resonances vs. Mn^{2+} concentration do not show any plateau.

4. Discussion

The understanding of molecular mechanisms of drug-membrane interaction has a practical importance for the design and the selection of new useful drugs. The aim of the present paper was to achieve a better understanding of the importance of medium pH on the MEA-membrane interaction.

The interaction between a very hydrophilic molecule like MEA and phospholipid bilayers has been shown previously [14,27–29]. Differential scanning calorimetry (DSC) and electron spin resonance (ESR) experiments had shown that the MEA location continuously fluctuates between the bulk water and the bilayer. This partitioning is pH-dependent and is ruled by a dynamic balance between the highly hydrophilic[NH_3^+] form and the less hydrophilic-NH_2 one at the lipid-water interface. This is supported by the existence of a pH at which an intralamellar dissociation balance occurs (as an apparent pK, noted pK_{app}), differing from the natural pK_a (10.35 [30,31]). For a 2:1 MEA/DPPC molar ratio, this pK_{app} is around 5.4 as revealed by membrane oxygen diffusion experiments [27,32] by spin labeling techniques in dipalmitoylphosphatidylcholine (DPPC) bilayers in L_α fluid phase. The 10.35 MEA pK_a value in pure water was confirmed by ^{15}N-NMR chemical shift changes vs. medium pH (not shown). In addition, pre-

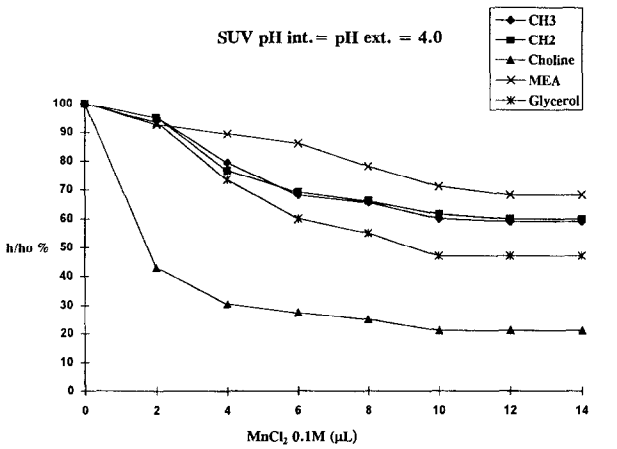

Fig. 7. Relative peak height reduction (%) of methyl (CH_3), methylene (CH_2), choline ($N^+(CH_3)_3$), glycerol (CH_2OCO) and MEA ^{1}H-NMR resonances in SUV plotted vs. $MnCl_2$ concentration. MEA resonances are poorly and progressively affected with $MnCl_2$ concentration.

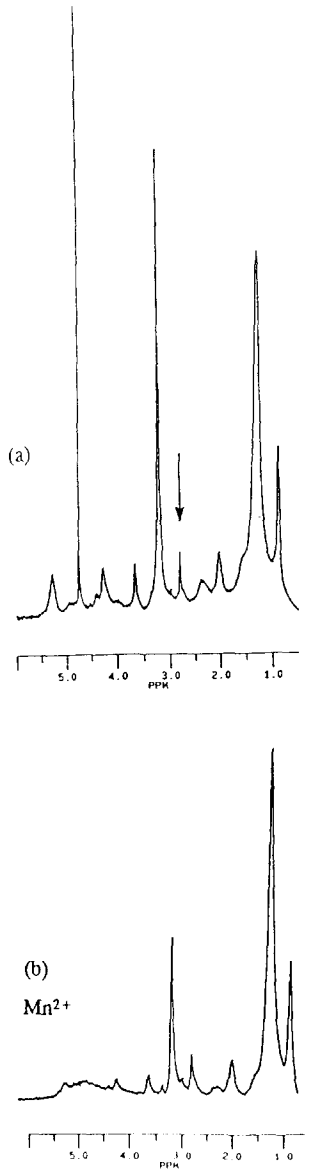

Fig. 8. 400 MHz ^{1}H-NMR spectra of MEA-containing SUVs. MEA/phospholipidids molar ratio of 1:4. Both spectra are recorded in presence of a pH gradient, initial $pH_{int} = 4.0$ and $pH_{ext} = 7.8$. Upfield MEA resonances are plotted with the arrow. Downfield resonances are lost in the $N^+(CH_3)_3$ peak. After 5 μl 0.1 M $MnCl_2$ addition (b), broadening of MEA resonance confirms the existence of a MEA-membrane interaction in presence of a pH gradient.

vious studies had revealed the existence of a new dissociation balance at the phospholipid–water interface, with labeled [^{15}N]DPPC and dipalmitoylphosphatidylethanolamine ([^{15}N]DPPE) [33,34].

For LUVs, ^{15}N-NMR recordings suggest a transmembrane transport of MEA in the presence or absence of pH gradient and even under acidic pH_{ext} (4.8). This result is rather unexpected because this very hydrophilic molecule is mostly ionized at this pH. These results confirm the existence of a pK_{app} lower than the pK_a value. Increasing pH_{ext} value promotes transmembrane crossing. The fact that the percentage of [^{15}N]MEA, no longer sensitive to Mn^{2+}, increases with the external pH value is consistent with a stronger pH-dependent interaction between MEA and the bilayer. In Figs. 2–4, the half-height widths ($\Delta\nu$) of the ^{15}N peak affected by Mn^{2+} significantly increases with the pH_{ext} value.

Fig. 5 shows that at a lower pH_{ext} value (4.8), Mn^{2+} eliminates MEA resonance by broadening beyond detection, while at higher pH_{ext}, MEA resonance is not completely suppressed but only broadened. This would argue for the existence of MEA populations, located either at the lipid–water interface, in the bilayer core, or in the intravesicular water bulk phase. Thus, a dynamic balance might occur between these different populations, since any MEA molecule would fluctuate between these different sites, according to the ionization state. Due to MEA size and membrane microviscosity, the MEA correlation time within the bilayer must be short, compared with the spectroscopic ^{15}N-NMR time scale. Conversely, exchanges between intra- and extravesicular MEA populations must be sufficiently slow to allow clear differentiation by ^{15}N-NMR spectroscopy.

At this stage, the existence of a MEA-bilayer interaction is obvious, but additional information is needed for more precision. Therefore, ^{1}H-NMR spectroscopy was used to examine the location of MEA in the SUVs bilayers.

The study of SUVs, the internal volume of which is much smaller than of LUV, show that MEA largely interacts with the bilayers. Large MEA resonances, visible in Fig. 6, confirm the existence of the MEA membrane interaction suggested by ^{15}N-NMR spectroscopy. Adding $MnCl_2$ to SUVs with initial pH_{int} and pH_{ext} equal to 4.0 shows that MEA resonances vs. $MnCl_2$ concentration are practically similar to the aliphatic methylene and methyl ones. This suggests the presence of MEA in the depth of the membrane, in the

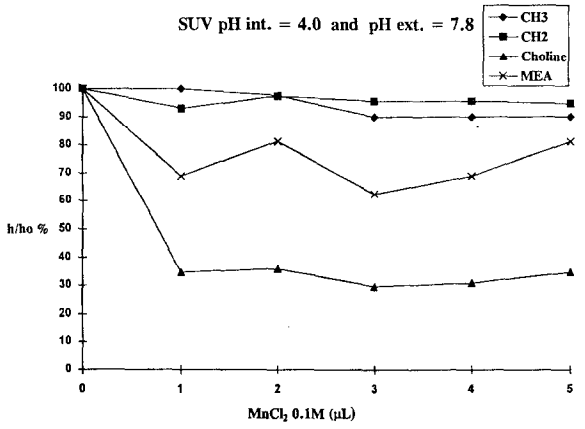

Fig. 9. Relative peak height reduction (%) of methyl (CH_3), methylene (CH_2), choline ($N^+(CH_3)_3$), and MEA ^{1}H-NMR resonances in SUV plotted vs. $MnCl_2$ concentration. MEA resonances are poorly but rapidly decreased with $MnCl_2$ concentration.

alkyl chain region. Besides, the broadening of MEA resonances when adding Mn^{2+} would indicate the presence of MEA between both layers.

It is noteworthy, in SUV experiments, that the consequences of Mn^{2+} addition are different when a pH gradient is present. In fact, ^{1}H-NMR spectroscopy of the protons located within the core of the bilayer such as $-CH_3$ and $-CH_2$ alkyl groups shows little, if any, changes in the presence of Mn^{2+}, perhaps due to repulsive positive charges (of Mn^{2+} and of the higher H^+ activity in the inner leaflet when pH_{ext} is higher than pH_{int}). In addition, the internal position of the $-CH_2$ and $-CH_3$ groups of the alkyl chains would limit the accessibility to Mn^{2+}. In the presence of a pH gradient, MEA seems more mobile and scattered within the bilayer, and even between both layers. This MEA mobility could be ascribed to a reorganization of SUV phospholipids under the effect of the external pH.

The studies carried out with ^{15}N- and ^{1}H-NMR spectroscopies discriminate between two MEA populations: intravesicular and extravesicular. An interaction between MEA and alkyl chains of the liposome membrane is also confirmed.

The results on both LUV and SUV model membranes are similar but complementary. LUV studies define the pH conditions favorable to the MEA transport across the bilayer. In LUV, ^{15}N-NMR gives valuable informations on MEA translocation between the internal and external spaces of the vesicle and its pH-dependence. Previous ESR studies had shown the alterations of the spin exchange between a fatty acid 16-nitroxide spin label and paramagnetic O_2, due to the presence of MEA within the inner core of the bilayer [27,28,32]. The present ^{15}N-NMR study on MEA transport across phospholipidic bilayers, beyond simple membrane interactions, could be generalized to all molecules possessing an amino group, such as amino acids, peptides or proteins.

5. Conclusion

^{31}P-NMR spectroscopy proved to be an efficient technique to study the membrane permeability of phosphorylated molecules such as nucleotides [5]. ^{1}H-NMR spectroscopy has been used to study the transport of aromatic compounds, such as purine analogues, which exhibit ^{1}H low field-shifted resonances [35]. ^{1}H-NMR spectroscopy study of MEA membrane crossing is unsuccessful for MEA resonances are hidden by the LUV broad resonances. On the contrary, SUV resonances are less broadened and MEA membrane interactions can be observed. SUV studies without a pH gradient, show that MEA locates in the depth of the membrane and, in presence of a pH gradient, presents a medial location, probably due to an increased mobility.

Further studies are in progress with a new class of signal peptides to analyze their interactions with phospholipidic model membranes and to find the proper physicochemical conditions for their translocation across membranes, also compatible with protein import.

Acknowledgements

This work was supported by a grant from the Direction des Recherches Etudes et Techniques. Contract no. 90/1073.

References

[1] Mayer LD, Bally MB, Cullis PR. Uptake of adriamycin into large unilamellar vesicles in response to a pH gradient. Biochim. Biophys. Acta 1986;857:123–126.

[2] Harrigan PR, Wong KF, Redelmeier TE, Wheeler JJ, Cullis PR. Accumulation of doxorubicin and other lipophilic amines into large unilamellar vesicles in response to transmembrane pH gradients. Biochim. Biophys. Acta 1993;1149:329–338.

[3] Chakrabarti AC, Clark-Lewis I, Cullis PR. Influence of charge, charge distribution, and hydrophobicity on the transport of short model peptides into liposomes in response to transmembrane pH gradients. Biochemistry 1994;33:8479–8485.

[4] Neumann JM, Hervé M, Debouzy JC et al. Synthesis and transmembrane transport studies by NMR of a glucosyl phospholipid of thymidine. J. Am. Chem. Soc. 1989;111:4270–4277.

[5] Henin Y, Goueytte C, Schwartz O, Debouzy JC, Neumann JM, Huynh-Dinh T. Lipophilic glycosyl phosphotriester derivatives of AZT: synthesis, NMR transmembrane transport study, and antiviral activity. J. Med. Chem. 1991;34:1830–1837.

[6] Debouzy JC, Hervé M, Neumann JM, Goueytte C, Dupraz D, Huynh-Dinh T. Glucosyl phosphotriesters of nucleosides: exchange mechanism of transmembrane transport and application to 5-fluoro-deoxyuridine. Biochem. Pharmacol. 1990;39:1657–1664.

[7] Lagoueyte C, Subra G, Bonnet PA et al. Synthèse de la [^{15}N]-cystéamine. J. Label. Compd. Radiopharm. 1993;33:711–716.

[8] Debouzy JC, Neumann JM, Herve M, Daveloose D, Viret J, Apizt-Castro R. Interaction of antiaggregant molecule ajoene with membranes: an ESR and ^{1}H-, ^{2}H, ^{31}P-NMR study. Eur. Biophys. J. 1989;17:211–216.

[9] Debouzy JC, Fauvelle F, Vezin H, Brasme B, Chancerelle Y. Interaction of the malonyldialdehyde molecule with membranes. A differential scanning calorimetry, ^{1}H-, ^{31}P-NMR and ESR study. Biochem. Pharmacol. 1992;44:1787–1793.

[10] Jendrasiak GL, Smith R, Ribiero AA. Chaotropic anion-phosphatidylcholine membrane interactions: an ultra high field NMR study. Biochim. Biophys. Acta 1993;1145:25–32.

[11] Bacq ZM, Hervé A, Lecomte J et al. Protection contre le rayonnement X par la β-mercaptoéthylamine. Arch. Intern. Physiol. 1952;59:442–447.

[12] Vachon A. Etude du transport de l'oxygène dans des membranes lipidiques modèles par marquage de spin en RPE. Apport à la radioprotection chimique. Application à l'étude des ginkgolides. Ph.D thesis, Université de Paris VI (1988).

[13] Berleur F, Roman V, Jaskierowicz D et al. The binding of the radioprotective agent cysteamine with the phospholipidic membrane headgroup-interface region. Biochem. Pharmacol. 1985;34:3071–3080.

[14] Roman V, Berleur F. Liposomes as carriers of cysteamine by the oral route. In: Gregoriadis, G. editors. Liposomes as Drug Carriers. Wiley, London, 1988:649–659.

[15] Roman V, Bocquier F, Leterrier F, Fatome M. Action radioprotectrice de la cystéamine encapsulée dans des liposomes administrés par voie orale à la souris. C.R. Acad. Sc. Paris 1982;295:191–193.

[16] Szoka F, Papahadjopoulos D. Procedure for preparation of liposomes with large aqueous space and high capture by reverse phase evaporation. Proc. Natl. Acad. Sci. USA 1978;75:4194–4198.

[17] Szoka F, Olson F, Heath T, Vail W, Mayew E, Papahadjopoulos D. Preparation of unilamellar liposomes of intermediate size by a combination of reverse phase evaporation and extrusion through polycarbonate membranes. Biochim. Biophys. Acta 1980;601:559–571.

[18] Hervé M, Debouzy JC, Borowski E, Cybulska B, Gary-Bobo CM. The role of the carboxyl and amino groups of polyene macrolides in their interactions with sterols and their selective toxicity. A ^{31}P-NMR study. Biochim. Biophys. Acta 1989;980:261–272.

[19] Hervé M, Goudeau M, Neumann JM, Debouzy JC, Goudeau H. Measurement of an intracellular pH rise after fertilization in crab eggs using ^{31}P-NMR. Eur. Biophys. J. 1989;17:191–199.

[20] Hauser H, Mantsch HH, Casal HL. Spontaneous formation of small unilamellar vesicles by pH jump: a pH gradient across the bilayer membrane as the driving force. Biochemistry 1990;29:2321–2329.

[21] Huang GC. Studies on phosphatidylcholine vesicles, formation and physical characteristics. Biochemistry 1969;8:344–352.

[22] Neumann JM, Zachowoki A, Tran-Dinh S, Devaux PF. High resolution proton magnetic resonance of sonicated phospholipids. Eur. Biophys. J. 1985;11:219–223.

[23] Hervé M, Cybulska B, Gary-Bobo CM. Cation permeability induced by valinomycin, gramicidin D and amphotericin B in large lipidic unilamellar vesicles studied by ^{31}P-NMR. Eur. Biophys. J. 1985;12:121–128.

[24] Neumann JM, Zachowski A, Tran-Dinh S, Devaux PF. High resolution proton magnetic resonance of sonicated phospholipids. Eur. Biophys. J. 1985;11:219–223.

[25] Trandinh S, Prigent Y, Lacapère JJ, Gary-Bobo C. An NMR method for the study of proton transport across phospholipid vesicles. Biochem. Biophys. Res. Commun. 1981;99:429–435.

[26] Chan SL, Feigenson GW, Seiter CHA. Nuclear relaxation studies of lecithin bilayers. Nature 1971;231:110–112.

[27] Vachon A, Roman V, Lecomte C, Folcher G, Fatome M, Braquet P, Berleur F. A radioprotector, cysteamine, inhibits oxygen transport in lipidic membranes. Int. J. Radiat. Biol. 1987;52:847–852.

[28] Bonnet PA, Roman V, Fatome M, Berleur F. Carboxylic acid or primary amine titration at the lipid-water interface: On the role of electric charges and phospholipid acyl chain composition. A spin labeling experiment. Chem. Phys. Lipids 1990;55:133–143.

[29] Bonnet PA, Berleur F, Roman V, Fatome M. Stearic acid pH-dependent reactivity in dipalmitoylphosphatidylcholine model membranes in Lβ' gel phase. J. Chem. Soc., Faraday Trans. 1987;1(83):177–190.

[30] Danehy JP, Noel CJ. The relative nucleophilic character of several mercaptans toward ethylene oxide. J. Am. Chem. Soc. 1960;82:2511–2515.

[31] Jocelyn PC. Biochemistry of the SH group. Academic Press, London, 1972, pp. 47–62.

[32] Vachon A, Lecomte C, Braquet P, Roman V, Fatome M, Berleur F. Oxygen diffusion-concentration in phospholipidic model membranes. J. Chem. Soc. Faraday Trans 1987;1(83):177–190.

[33] Akoka S, Tellier C, Poignant S. Molecular order, dynamics, and ionization state of phosphatidylethanolamine bilayers as studied by ^{15}N NMR. Biochemistry 1986;25:6972–6977.

[34] Akoka S, Tellier C. Calcium and spermine interaction with phospholipid bilayers: A ^{15}N NMR study. Biochimie 1989;71:137–144.

[35] Debouzy JC, Gueiffier A, Fauvelle F, Viols H, Dejean E, Neirinck V, Peinnequin A, Bachelet C, Perly B, Chapat JP. Synthetic pyridopurines derived from food pyrolysis products: intercalation, interactions with membranes, cyclodextrin complexation, and biological mitogenic properties. J. Pharm. Sci. 1996;85:200–205.